Int. J. Electrochem. Sci., 12 **(2017)** 3732 – 3740, doi: 10.20964/2017.05.54

International Journal of ELECTROCHEMICAL SCIENCE
www.electrochemsci.org

Preparation of Au nano-tips for *in-situ* Investigation of Early-Age Localized Corrosion of Three Metals by Scanning Electrochemical Microscope

Huan Hao[1], *Chaodi Xu*[1], *Yongxin Li*[1,3,*], *Emily Jackson*[3], *Xianming Shi*[2,*]

[1] College of Chemistry and Materials Science, Anhui Normal University, Wuhu 241000, China
[2] Laboratory of Corrosion Science & Electrochemical Engineering, Department of Civil and Environmental Engineering, Washington State University, Pullman, WA 99164-2910;
[3] Corrosion and Sustainable Infrastructure Laboratory, Western Transportation Institute, PO Box 174250, College of Engineering, Montana State University, Bozeman, MT 59717-4250, USA
[*]E-mail: yongli@mail.ahnu.edu.cn, xianming.shi@wsu.edu

Received: 14 February 2017 / *Accepted:* 28 March 2017 / *Published:* 12 April 2017

In this work, scanning electrochemical microscopy (SECM) was employed for corrosion studies of carbon steel, stainless steel and aluminum alloy in a neutral chloride solution. The SECM Au tips at nano-scale size were prepared by laser-assisted pulling method and characterized by scanning electron microscope (SEM) and electrochemical method. In the SECM test, the I^-/I_3^- redox couple was used as a mediator for mapping the temporal and spatial evolutions of tip current on each metallic substrate with or without a scratched nanocomposite coating. The results reveal that it is appropriate to combine the generation-collection (G-C) mode of SECM with the feedback current mode in order to elucidate the possible reaction mechanism and pathways underlying the localized corrosion of the three metals investigated.

Keywords: Stainless steel; carbon steel; aluminum alloy; localized corrosion; scanning electrochemical microscope (SECM)

1. INTRODUCTION

It is crucial to characterize and understand the localized electrochemical reactions on metal surfaces, for corrosion science and engineering applications [1-3]. Generally, steady-state polarization curves and electrochemical impedance spectroscopy (EIS), served as the conventional electrochemical techniques, are commonly used for studying the corrosion current and / or the corrosion rate on the surface [4]. However, all of those are integral methods, which fail to provide the spatial resolution

needed to illustrate the degradation process especially in the early stage of metallic corrosion. As such, these methods do not enable in-depth understanding of mechanistic details critical to localized corrosion, such as those associated with the initiation and propagation of pits on bare metals and the coating delamination in the vicinity of defects on coated metals.

Recent years have seen significant studies towards better understanding of localized corrosion forms, especially during their early stage. These generally focus on the determination of localized chemistry during the localized corrosion processes, from a surface science perspective. Several significant local electrochemical scanning techniques have been developed and applied in electrochemical and corrosion sciences, such as scanning reference electrode technique (SRET) [5], scanning Kelvin probe (SKP) [6], electrochemical microcell technique [7], and scanning electrochemical microscope (SECM) [8-10]. Among them, SECM is a powerful technique for detecting various electrochemical reactions in the corrosion process, through the characterization of the metal /solution interface morphology and redox activity. SECM features outstanding electrochemical sensitivity and high spatial resolution [8-10]. It consists of a three-dimensional moving ultramicroelectrode, which is immersed in an electrolyte solution and scans the surface close to the solid base. Thus, the SECM tip can be employed for quantitative detection of reactants and products involved in corrosion reactions. One limitation is that most of the previous works used commercial Pt micro-size tips to record the SECM image, which are expensive and have relatively low spatial resolution. Theoretically, the much higher resolution images could be obtained if the tips were smaller during SECM test, and the early-age localized corrosion could be observed through the high-resolution SECM images.

It is well-known that the surface of Au electrode has more reaction activity than that of other metal electrodes such as Pt electrode, but the fabrication of single Au nanoelectrodes is still a challenge due to the relative low melting point of Au [11]. In this work, Au nano-sized tips were fabricated by laser-assisted method as reported in our previous work [11, 12], and then characterized by scanning electron microscope and electrochemical methods. For the first time, the prepared Au nano-tips were used to image the localized corrosion of carbon steel, stainless steel and aluminum alloy in a neutral chloride solution. An I^-/I_3^- redox couple is used as the mediator for mapping the temporal and spatial evolutions of tip current on different metallic substrates (carbon steel, stainless steel and aluminum alloy), and the experimental results reveal that stainless steel has the best performance in corrosion resistance.

2. EXPERIMENTAL

2.1. Chemicals and materials

ZPA (Zinc Aluminum Phosphate) was a proprietary corrosion inhibitor obtained from Montana State University. The epoxy resin ANCAREX AR555 and ANQUAMINE 419 (Air Products and Chemicals, Inc., PA, USA), Nano-Fe_2O_3 (MTI Corporation, Richmond, CA, USA), Multi-wall carbon nantubes (CNTs) and NC 7000 (Nanocyl^{TM}, Belgium), Non-modified montmorillonite (Nano-clay)

and polysiloxane-modified montmorillonite (PS-clay) (Nanocor. Inc., Hoffman Estates, IL, USA) were purchased without further treatment. The aluminum alloy coupons and steel purchased from Cultural Co. (Gaoyou, Jiangsu, China), and the parameter details can be found in our previous work [13].

Analytical-grade chemicals and twice- distilled water was be used to prepare the solution of 100 mM NaCl + 10 mM KI, which were considered an electrolyte solution. All measurements were carried out in a natural aerated solution at ambient temperature.

2.2. Apparatus and Methods

2.2.1. Apparatus

All SECM scans and electrochemical measurements were performed on a CHI900C electrochemical workstation (CHI instrument, Shanghai, China). An Ag/AgCl electrode was utilized as a reference electrode and a looped Pt wire was used as a counter electrode. The electrochemical cell with a specimen press fitted at its bottom hole was mounted on the three-axis translation stage. Specimen was mounted horizontally facing upwards. The Pt tips were used at a height of 40 μm above the specimen surface during the SECM measurements.

2.2.2. Fabrication of Au Tips.

The fabrication of Au tips using laser-assisted pulling method involves three-step process as previously described.[11, 12] Briefly, an ultra-sharp Au nanowire tip (<10 nm) was first pulled from a Au microwire using a laser puller (P-2000, Sutter). The Au nanowire tip was visualized using a 400× magnification microscope (Olympus, BX51). Ultra-sharp borosilicate capillary/Au tip was polished by a BV-10 Beveler (Sutter Co., USA).

2.3. Steel substrate treatment

The copper wires were attached to the surface of each cylindrical steel test coupons and sealed with waterproof marine epoxy to cover all surfaces except the surface exposed to the electrolyte. After curing of the epoxy resin, the unsealed sample surface was polished on silicon carbide (SiC) paper to a mesh size of 1000 by means of a metallographic abrasive disk. After polishing, the surface of the sample was rinsed with tap water, then sonicated in deionized water and rinsed with acetone again.

2.4. Coating preparation

Epoxy nanocomposites were generally prepared through dispersing the nanomaterials into an epoxy matrix using a solvent or heating method. But it was found that heating method was liable to cause clustering or aggregation of the nanomaterials, and the dispersibility was poor. The use of solvents could help disperse nanomaterials in the resin. However, it was found that the curing agents

were usually added to the mixture after removal of the solvent by vacuum evaporation. This tends to disrupt the uniformity of the cured nanocomposite, particularly when loaded with high nanomaterials. In order to avoid this issue, the curing agent could be added to the mixture prior to removal of the solvent to improve the dispersion of the nanomaterial in the coating. Moreover, the slurry may be applied directly on the surface of the metal substrates to form a uniform thin barrier coating.

In this process, the resin and the curing agent were diluted with water with the weight ratio of 1: 1 respectively, before being mixed. Various percentages of nanomaterials were added to the resin/water solution followed by vigorous stirring (Model 14-503, Fisher Scientific, Inc., USA), and then the solution was sonicated (Model 50T, VWR, West Chester, PA, USA) for 10 minutes. After that, the hardener-aqueous solution was added to the mixture, followed by stirring and sonication again for 10 minutes. The steel substrate was immersed into the final prepared mixture for just 1 minute. For facilitate initial curing, the coated samples were placed in an oven at 40 °C for over 24 hours. Finally, the coated samples were cured for additional 6 days at ambient temperature and humidity (~ 21°C, and ~50% relative humidity) to form a uniform coating for corrosion testing and surface analysis in this experiment.

After previous morphological studies and electrochemical tests, sample # 10, which has the best performance for anti-corrosion, was selected to do SECM test.

3. RESULTS AND DISCUSSION

3.1. Characterization of Au nano-tips

After Au nano-tips were prepared through laser-assisted pulling and polishing process, their SEM images were taken, which were showed in Figure 1(a). From Figure 1(a), it can be seen that the prepared Au nano-tips are longer in length and have a sharper end. After polishing, Au nanowire can be observed on the disk-type, flat geometric surface (data no shown). To further identify the Au nano-tips, a typical cyclic voltammogram was recorded in a 0.5 M H_2SO_4 solution, as shown in Figure 1(b). The anodic peak appeared at ~1.2 V and the cathodic peak appeared at ~ 0.9 V may be attributed to Au oxide formation and its reduction, respectively [14].

Meanwhile, the voltammetric responses by use of Au nano-tips were recorded in Fc, $K_3Fe(CN)_6$ and $Ru(NH_3)_6Cl_3$ solutions, respectively, as shown in Figure 2. From Figure 2, it could be obtained that all the voltammograms from Fc, $K_3Fe(CN)_6$ and $Ru(NH_3)_6Cl_3$ have ideal sigmoidal shape and no obvious hysteresis could be found on the reverse scan, suggesting that the tip is sealed very well by glass during the pulling and polishing process. The radii of the nano-tips can be calculated from the following equation by measuring the diffusion-limited steady-state current assume the surface is disk-shape.

$$i_{ss} = 4nFDC_br \quad (1)$$

where n is the numbers of electrons transferred per molecule, F is the Faraday's constant, and D and C_b are the diffusion coefficient and bulk concentration of the redox molecule, respectively. The

radius of Au tips used in this experiment for SECM image can be obtained based on *eq. 1*, which is ~ 220 nm, as shown in Figure 2.

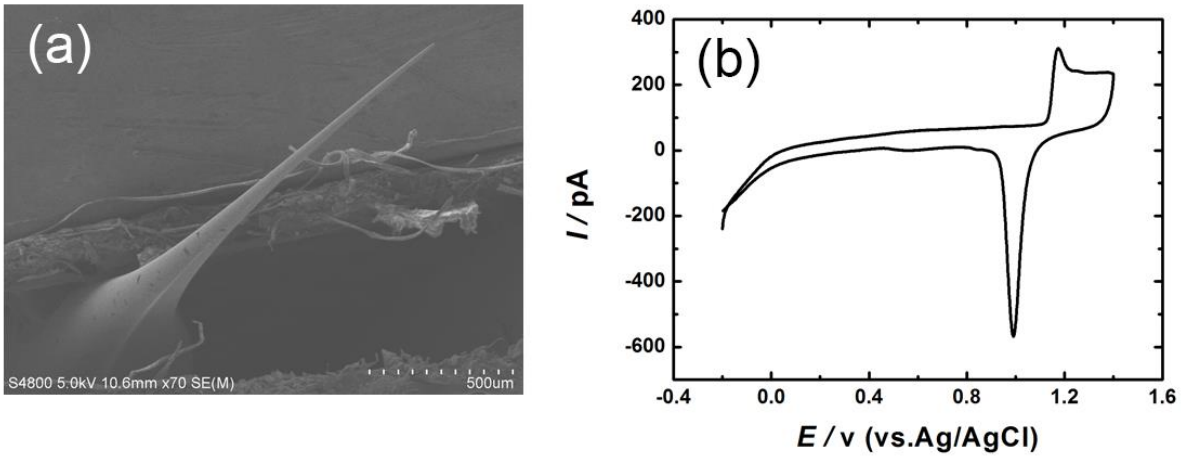

Figure 1. (a) SEM image of a polished Au nanotip. (b) The cyclic voltammograms of Au nanotip in a 0.5 M H_2SO_4 solution with the radius of ~ 230 nm.

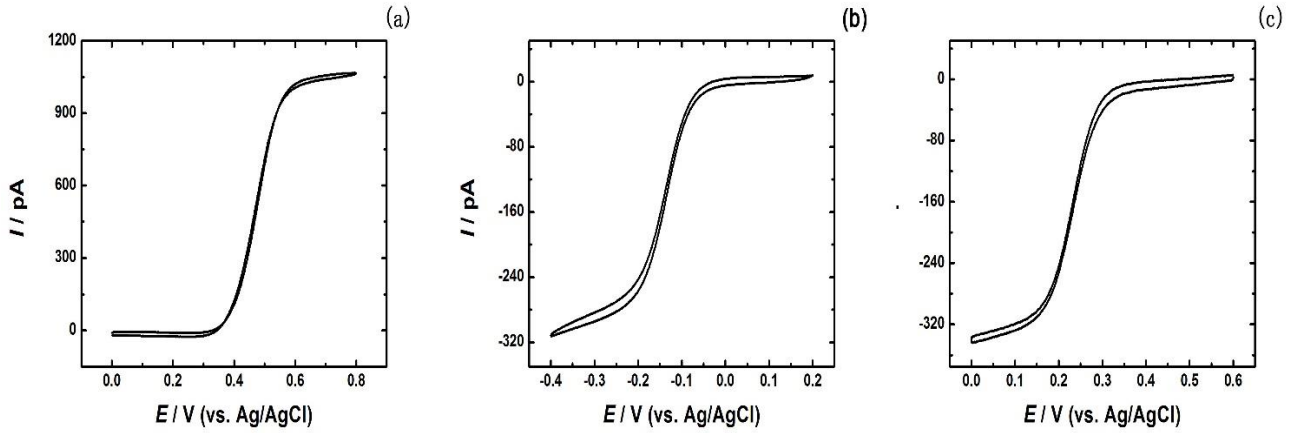

Figure 2. Votammetric responses of Au nano-tip in a ACN solution containing 5 mM Fc and 0.2 M $TBAPF_6$ (a), an aqueous solution containing 5mM $Ru(NH_3)_6Cl_3$ and 0.2 M KCl (b), and an aqueous solution containing 5 mM $K_3Fe(CN)_6$ and 0.2 M KCl (c).

3.2. SECM Images for bare metal coupons

The prepared Au nano-tips were used to image the surface corrosion. The SECM images of bare stainless steel at the area of 500 × 500 μm in a 100 mM NaCl + 10 mM KI solution with different immersion times were tested, and the results are shown in Figure 3. From Figure 3a, it is evident that almost no tip current appeared when the stainless steel was immersed into the above solution, suggesting the corrosion process was not taken place. However, the contour plot clearly appeared from Figure 3b,3c and 3d, indicating that Fe^{2+} is locally generated above the defect, and the size and shape of the peak current changed with the immersion time. According to previous result [15, 16], the reaction mechanism on the tip and the substrate surface can be given as follows:

Dissolution reaction on substrate: $Fe - 2e^- \rightarrow Fe^{2+}$ (1)

Reaction on tip: $Fe^{2+} - e^- \rightarrow Fe^{3+}$ (2)

$3I^- - 2e^- \rightarrow I_3^-$ (3)

Surface reaction on substrate:

$Fe^{2+} + I_3^- \rightarrow Fe^{3+} + 3I^-$ (4)

Fe^{2+} ions could be appeared if the pitting corrosion at the initial stage took place on the coupon surface (reaction 1), which then would be oxidized to Fe^{3+} ions on the tip (reaction 2). At the same time, I_3^- ions could be produced through the oxidation of I^- ions on the tip (reaction 3). In addition, it should be noted that, in addition to the dissolution reaction 1 and tip reaction 2 happened through the substrate generation-tip collection (SG-TC) mode which was assumed to be associated with the occurrence of pitting corrosion, the I_3^- ions generated at the tip (reaction 3) could be reduced to I^- ions by Fe^{2+} ions (reaction 4). The produced I^- ions would diffuse and feed back to the tip, and then were oxidized to I_3^- again. Therefore, the current on the tip was found to increase and obvious current maps of the pitting corrosion on the coupon surface could be observed.

At the beginning of immersion, a single sharp current peak could be found on the coupon surface, showing that the sites of the coupon surface were readily attacked by chloride ions and the feedback current from the redox mediator could be observed. Subsequently, pitting corrosion induced by localized anodic dissolution was proved on the surface of the stainless steel samples, which could result in a high ratio of the depth width of the pit. In addition, it was found that the shape, size and quantity of the faradic current increased significantly with the increase of the immersion time (see Figure 3b, 2c and 2d), indicating the pitting corrosion can take place continuously with the immersion time.

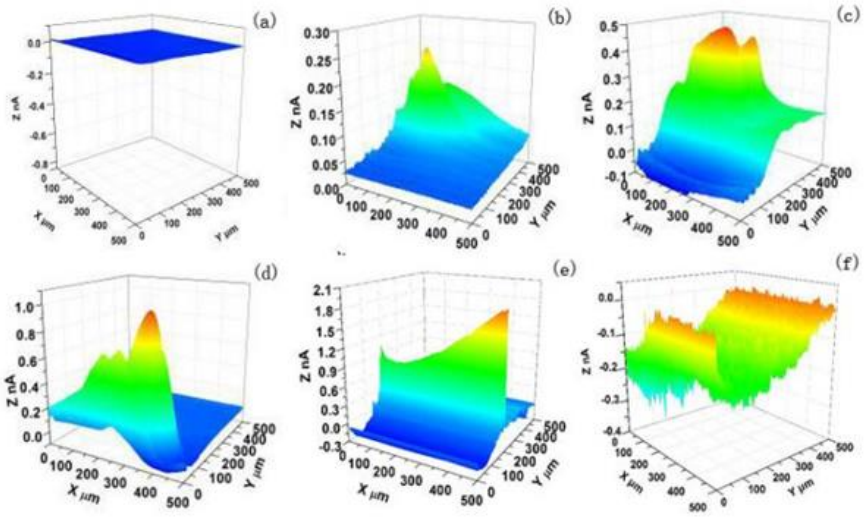

Figure 3. SECM images obtained for bare stainless steel in 3% NaCl solution + 10 mM KI with the immersing time of 0h (a), 4h (b), 12h (c) and 24h (d); SECM images obtained for bare carbon steel (e) and aluminum alloy (f) immersed in 3% NaCl solution + 10 mM KI for 8 h and 24 h, respectively.

The SECM images of bare carbon steel and aluminum alloy at the area of 500 × 500 μm in a 100 mM NaCl + 10 mM KI solution were also measured, and the results are shown in Figure 3. From Figure 3e, it could be found that the value of tip current collected from carbon steel was much larger than that from stainless steel (see Figure 3d) though the immersing time was just 8 hours, indicating stainless steel has excellent anti-corrosion property in the investigated electrolyte. However, the value of tip current shown in Figure 3f collected from aluminum alloy was much smaller than that from stainless steel (see Figure 3d), which may be due to the lack of feedback current from aluminum alloy substrate.

3.3. SECM Images for epoxy-nanocomposite coated metal coupons

To investigate the anti-corrosion property of epoxy-nanocomposite coated metal coupons, the SECM images epoxy-nanocomposite coated stainless steel at the area of 500 × 500 μm in 100 mM NaCl + 10 mM KI solution with different immersion times were tested, and the results are shown in Figure 4. As mentioned above, the reactions took place on the tip/substrate are the same (reaction 1 to reaction 4), the only difference between Figure 4 and Figure 3 is the epoxy-nanocomposite coating layer.

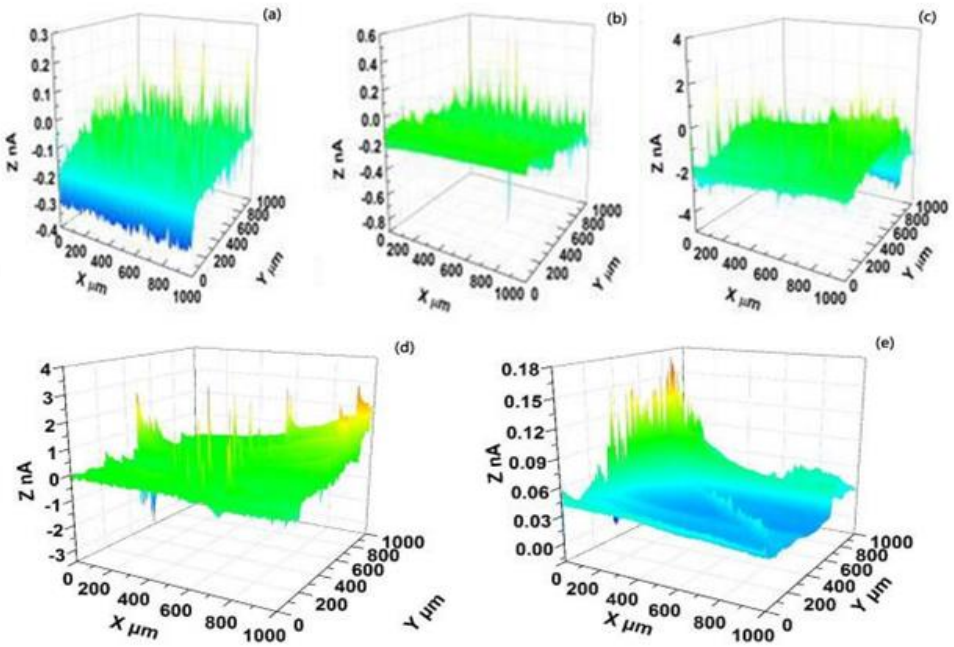

Figure 4. SECM images obtained for epoxy-nanocomposite coated stainless steel in 3% NaCl solution + 10 mM KI with the immersing time of 4h (a), 12h (b), and 24h (c). SECM images obtained for epoxy-nanocomposite coated carbon steel (d) and aluminum alloy (e) immersed in 3% NaCl solution + 10 mM KI for 24 h.

From Figure 4a, b and c, it can be observed that there are only some small lines appeared, and the size and shape of the tip current are much smaller than that shown in Figure 3a, b, c and d, even the immersing time is reached to 24 hours, indicating the epoxy-nanocomposite coating layer has good

anti-corrosion property, but pitting corrosion still can happen the surface of the stainless steel. For comparison, the SECM images of epoxy-nanocomposite coated carbon steel and aluminum alloy were also provided in Figure 4d and e. It can be observed that the value of tip current from carbon steel is larger than that collected from stainless steel (Figure 4c) whereas the value is much smaller than that collected from aluminum alloy (Figure 4e), indicating that carbon steel is easily attacked by chloride ions and formed pitting corrosion, but aluminum alloy is underwent a different reaction mechanism.

Based on the SECM images shown in Figure 4 and our previous result[17], it can be obtained that the nanomaterials can improve the anti-corrosion property of the cured epoxy resin coating, reduce the surface porosity of the coating matrix, and cause the diffusion path of the hazardous substance to be zigzagged, which can lead to the improvement of barrier properties of the epoxy coating. Meanwhile, nanomaterials could improve the adhesion of the cured epoxy coating to the underlying steel substrate and alter the physiochemical properties of the interface between coating layer and steel substrate. From above discussion, it could be obtained that our prepared Au nano-tips was suitable to be employed as SECM tips to in situ monitor the early-age localized corrosion of three metals in a in a 3% NaCl + 10 mM KI solution. Many works have been reported for investigating localized corrosion in steels and aluminum couples by use of commercial Pt microelectrodes [8, 18-24]. For example, Bastos et al. used 10 μm platinum tip to detect the release of ferrous ions at the anodic sites and the consumption of dissolved oxygen at the cathodic sites at the open-circuit potential in an aerated aqueous solution of 0.1 M NaCl [8], Garcia et al. also investigated the metastable pitting on austenitic stainless steel at the open-circuit corrosion potential using scanning electrochemical microscopy with 10 μm platinum tip [23]. Eckhard et al. found that tiny corrosion pit was generated by inducing active corrosion underneath an accurately positioned 5 μm diameter Pt disk SECM tip that served as counter electrode in the direct mode of SECM [22]. Luong et al. used 10 μm platinum tip to detect pitting precursor sites of pure iron in a solution of 50 mM NaCl at pH 8.4 through collecting the Fe^{3+} ions released from the corroding surface [24]. Compared with previous work, the proposed Au nano-tip used for SECM has its advantage: the radii were easily size-tunable through the common polishing process, and the cost is low, which is important for SECM application because the tips are frequently broken during the approaching process. Theoretically, the much higher resolution images could be obtained if the tips were smaller during SECM test, and the early-age localized corrosion could be observed through the high-resolution SECM images, and related works are in progress in our group.

4. CONCLUSIONS

In this communication, Au nano-tips were prepared by laser-assisted pulling process and characterized by SEM and cyclic voltammetries. The Au nano-tips coupled with the SECM technique were used to investigate the early-age localized corrosion of three metals (stainless steels, carbon steel and aluminum alloy substrates without with an epoxy-nanocomposite coating) in a 3% NaCl + 10 mM KI solution. The shape and size of the current peaks in the SECM scan region image significantly changed with the increase of the immersing time, indicating the process of initiation and growth of localized corrosion at the defective sites of passivated films. The results reveal that stainless steel has the best performance in corrosion resistance regardless of the presence of an epoxy-nanocomposite

coating layer. This research shows that the combinate the feedback current model and the SECM's generation-collection (G-C) model is applicable to shed light on possible reaction mechanisms and pathways for localized corrosion of stainless steel, carbon steel and aluminum alloys in a neutral chloride solution. Due to the tunable size and low cost of the home-made SECM tips, it is possible to get much higher resolution images during SECM test, which can reveal the early-age localized corrosion of metals.

ACKNOWLEDGEMENTS.
This work is financially supported by the National Natural Science Foundation of China (No.21375002), the Key Project of Chinese Ministry of Education (No. 212083) and the Foundation for Innovation Team of Bioanalytical Chemistry of Anhui Province.

References

1. E. Ghali, W. Dietzel and K.-U. Kainer, *J. Mater. Eng. Perform.*, 13 (2004) 517.
2. I. Annergren, D. Thierry and F. Zou, *J. Electrochem. Soc.*, 144 (1997) 1208.
3. J. R. Xavier and R. Nallaiyan, *Journal of Failure Analysis and Prevention*, 16 (2016) 1082.
4. B. J. Little, R. I. Ray, P. A. Wagner, J. Jones‐Meehan, C. C. Lee and F. Mansfeld, *Biofouling*, 13 (1999) 301.
5. K. R. Trethewey, D. A. Sargeant, D. J. Marsh and A. A. Tamimi, *Corros. Sci.*, 35 (1993) 127.
6. G. Bäck, A. Nazarov and D. Thierry, *Corrosion*, 61 (2005) 951.
7. O. Guseva, J. A. DeRose and P. Schmutz, *Electrochim. Acta*, 88 (2013) 821.
8. A. C. Bastos, A. M. Simões, S. González, Y. González-García and R. M. Souto, *Electrochem. Commun.*, 6 (2004) 1212.
9. L. Niu, Y. Yin, W. Guo, M. Lu, R. Qin and S. Chen, *JMatS*, 44 (2009) 4511.
10. Y. Yin, L. Niu, M. Lu, W. Guo and S. Chen, *Appl. Surf. Sci.*, 255 (2009) 9193.
11. Y. Y. Zhang, S. Xu, Y. Y. Qian, X. S. Yang and Y. X. Li, *Rsc Advances*, 5 (2015) 77248.
12. Y. Li, D. Bergman and B. Zhang, *Anal. Chem.*, 81 (2009) 5496.
13. M. H. Nazari, X. Shi, E. Jackson, Y. Zhang and Y. Li, *J. Mater. Civil Eng.*, 29 (2017) 04016187.
14. K. Dawson, J. Strutwolf, K. P. Rodgers, G. Herzog, D. W. M. Arrigan, A. J. Quinn and A. O'Riordan, *Anal. Chem.*, 83 (2011) 5535.
15. X. He and X. Shi, *Transport. Res. Rec.: Journal of the Transportation Research Board*, 2070 (2008) 13.
16. T. E. Lister and P. J. Pinhero, *Electrochim. Acta*, 48 (2003) 2371.
17. X. Shi, T. A. Nguyen, Z. Suo, Y. Liu and R. Avci, *Surf. Coat. Technol.*, 204 (2009) 237.
18. B. M. Fernandez-Perez, J. Izquierdo, S. Gonzalez and R. M. Souto, *J. Solid State Electrochem.*, 18 (2014) 2983.
19. J. Izquierdo, A. Eifert, C. Kranz and R. M. Souto, *Chemelectrochem*, 2 (2015) 1847.
20. S. S. Jamali, S. E. Moulton, D. E. Tallman, M. Forsyth, J. Weber and G. G. Wallace, *Corros. Sci.*, 86 (2014) 93.
21. H. Luo, C. Dong, S. Gao, C. Du, K. Xiao and X. Li, *Rsc Advances*, 4 (2014) 56582.
22. K. Eckhard, M. Etienne, A. Schulte and W. Schuhmann, *Electrochem. Commun.*, 9 (2007) 1793.
23. Y. González-García, G. T. Burstein, S. González and R. M. Souto, *Electrochem. Commun.*, 6 (2004) 637.
24. B. T. Luong, A. Nishikata and T. Tsuru, *Electrochem. Commun.*, 71 (2003) 555.